Characterizing the Temporal Patterns of Travel Production: A Bird's Eye View of the Urbanization Levels in The Netherlands

Zahra Eftekhar*[1], Adam Pel[1], and Hans van Lint[1]

[1]Department of Transport & Planning, Delft University of Technology, The Netherlands

SHORT SUMMARY

This paper explores the temporal patterns in travel production using a full month of production data from traffic analysis zones (TAZ) in the (entire) Netherlands. This data is a processed aggregated derivative (due to privacy concerns) from GSM traces of a Dutch telecommunication company. This research thus also sheds light on whether such a processed data source is representative of both regular and non-regular patterns in travel production. To this end, the weekly patterns of hour-by-hour travel production of over 1200 TAZs are clustered using inception convolutional neural networks with k-mean methods. A silhoutte score shows that three dominant clusters can be discerned. Each cluster shows different within-day and day-to-day patterns in production. Furthermore, a spatial analysis of these clusters shows that they are related to urbanization levels: Urban, Rural, and mixed group. The findings of this study provide further insights in mobility, relevant for transportation analysis and policies.

Keywords: travel production; spatiotemporal; demand pattern; urbanization; temporal pattern.

1. INTRODUCTION

Understanding the travel demand patterns is essential for transportation planning and management. Firstly, travel demand analysis plays a significant role in identifying the current problems of transportation systems and helps in modeling the future traffic state (Thakuriah, 2001). Secondly, the demand patterns help evaluate the impact of transportation infrastructure and management policies and strategies, such as flexible-time work schedules and congestion pricing (Gärling et al., 2002). Thirdly, understanding demand patterns is useful to develop better standards for evacuation plans and responses (Xu, Chen, & Yang, 2017).

Travel demand includes noticeable spatial-temporal heterogeneity, as the amount of travel differs strongly across areas as well as time-of-day and day-of-week (Shen, Zhou, Jin, & Wang, 2020). Temporal variability is especially significant when modeling motor vehicle demand in urbanized areas where morning and afternoon peaks account for almost 50% of daily travel demand (Lin & Shin, 2008). Spatial heterogeneity is derived from diverse urbanization levels, economic activities, lifestyles, transportation accessibility, and resource distribution between areas e.g., (Fotheringham, Charlton, & Brunsdon, 1998). This spatial-temporal heterogeneity, including the identification of patterns therein, is an important part of understanding travel demand.

Many studies analyze the relationship between travel demand and land-use properties using methods based on Ordinary least squares (OLS) (Yang et al., 2018; Maat & Timmermans, 2006). However, OLS generally assumes homogeneous regression relationships, neglecting the spatial variation of the data. Overlooking spatial-temporal heterogeneity gives rise to some serious errors, for instance, misinterpretation of coefficients and inaccuracy in estimations (Anselin & Griffith, 1988).

To account for spatial heterogeneity, many extended OLS-like models have been developed amongst which the geographically weighted regression (GWR) model (Brunsdon, Fotheringham, & Charlton, 1996) that is widely used in transportation studies. For example, Cardozo, García-Palomares, and Gutiérrez study the relationship between transit travel demand and land use mix, bus accessibility, and road density using a GWR model. Whereas the GWR model can sufficiently describe spatial heterogeneity, it does not address temporal heterogeneity. Typically, days are divided into multiple periods, in which average (proportional) values are considered for modeling.

To incorporate temporal heterogeneity, a geographically and temporally weighted regression (GTWR) method to predict transit travel demand was first applied by (Ma, Zhang, Ding, & Wang, 2018). However, little is still known about how different areas have various spatiotemporal patterns in travel production associated with their urban development. There is a need to understand the factors that mediate the interactions between urbanization and travel production in time and space.

Fekih et al. proposes a framework to extract spatiotemporal travel demand patterns from large-scale GSM traces. Their analysis focuses on within-day variations of travel demand. In this paper we build on this work and investigate both within-day and day-to-day production patterns of all the traffic analysis zones (TAZs) in the Netherlands. The performed temporal analysis of the underlying patterns is valuable for adjusting the demand models and prediction. Later we link these temporal patterns to spatial urbanization levels which is beneficial for urban development strategies and policy makers. In fact, this study proposes three urbanization levels for the Netherlands: urban, rural, and other. Each level is characterized by its specific travel production pattern within-day and day-to-day, and this study explores the differences in these patterns. This effort is the first step to understanding the link between urbanization level and production patterns.

The remainder of this paper is organized as follows: Section 2 describes the research data and the implemented method. In Section 3, we present the results of our analysis on the temporal patterns found in the Netherlands. Finally, Section 4 concludes the paper.

2. METHODOLOGY

In this research, the hourly production of the 4-digit postal code zones in the entire Netherlands during March 2017 is used. Travel production of TAZ i is defined as the number of inter-zonal trips starting at i. The production values are derived from the GSM traces of a Dutch telecommunication company accounting for one third of all mobile phone users.

To better characterize the main production patterns, three distinct temporal clusters are presented and analyzed. A deep convolutional neural network (DCNN) based on transfer learning is applied for feature extraction. Finally, the K-means algorithm clusters the patterns.

Data description

This research explores in the hourly travel production data of motor vehicles in March 2017 of the 1246 TAZs in the entire Netherlands (see figure 1). The data source is a processed form of GSM traces of a telecommunication company, namely Vodafone, whose market share is about one-third of the Dutch population. Another company performed the processing due to privacy concerns of the raw mobile phone data. Consequently, the available data for this study, instead of the mobile phone traces, consists of origin-destination (OD) matrices of the motor vehicles based on TAZs in the Netherlands. These OD matrices have been initially scaled up to the entire Dutch population.

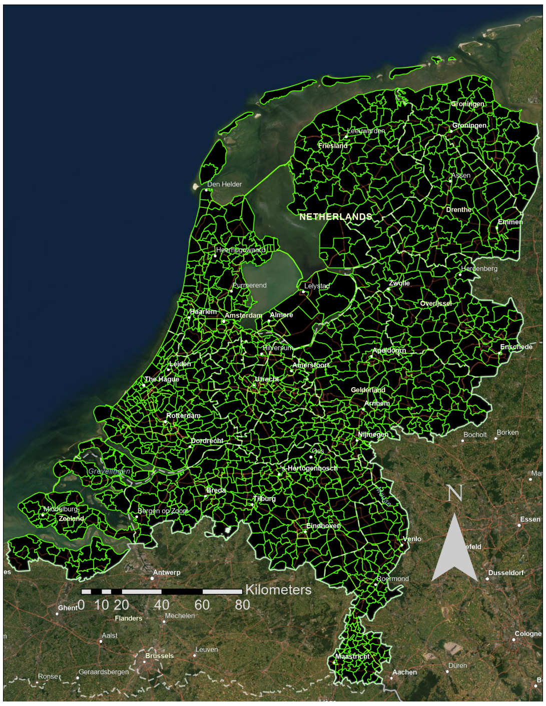

Figure 1: TAZs in the Netherlands.

For more detail on scaling procedure, we refer the reader to (Meppelink, Van Langen, Siebes, & Spruit, 2020).

To begin with, we collected the processed data. After pre-processing and reshaping, each zone had a heatmap of normalized production values. Normalizing the production values enables fast and stable pattern comparison of various zones. The technique we applied on each production value x for normalizing is Min-Max Scaling, i.e.,

$$x_{normalized} = \frac{x - x_{min}}{x_{max} - x_{min}} \tag{1}$$

where, $x_{normalized}$ is the normalized value, x_{min} and x_{max} are the minimum and maximum production values in the time series of each TAZ. The resulting normalized values range between 0 and 1.

The horizontal and vertical axes represent the days of the month and the hours of a day, respectively. Figure 2 shows an example. This representation allows us to see the temporal patterns of production both within a day and between days. Then we used the state-of-the-art InceptionV3 based on transfer learning with the K-means method (Szegedy, Vanhoucke, Ioffe, Shlens, & Wojna, 2016; Cohn & Holm, 2021; Van Gansbeke, Vandenhende, Georgoulis, Proesmans, & Van Gool, 2020) to cluster heatmaps.

K-means clustering

The K-mean clustering method splits the N-dimensional data set of M points (heatmaps) into K clusters such that the sum of the pairwise Euclidean distance between the points of each cluster is minimized (Hartigan & Wong, 1979). In other words, the objective of this method is to maximize the similarity between the points in the same cluster and maximize the dissimilarity of points from different clusters. Initialization of the method is by selecting K points randomly as the cluster centroids. The clustering process has two significant steps:

- **Assignment:** assigning each point to its closest centroid. Mathematically this step refers

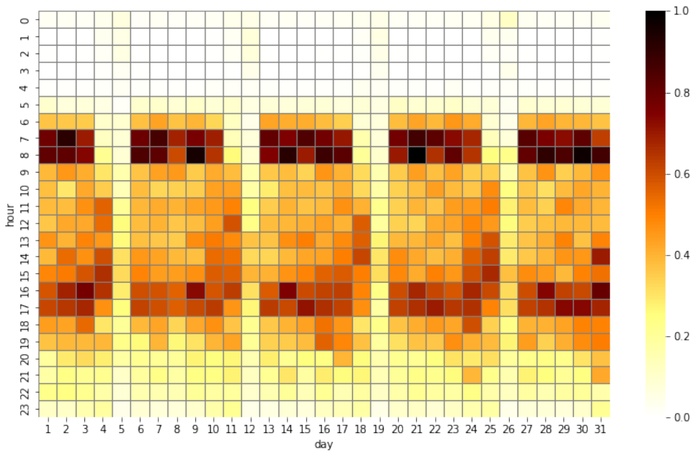

Figure 2: An example of production heat map for one zone.

to partitioning the points to the Voronoi diagram (Shamos & Hoey, 1975) generated by the centroids.

- **Update:** updating each cluster center to be the average of all points contained within them.

Deep convolutional neural network (DCNN)

The K-means clustering method, due to its easy application and effectiveness, is one of the most popular algorithms for clustering analysis (Poteraş, Mihăescu, & Mocanu, 2014). However, this method is inherently a linear algorithm (Ning & Hongyi, 2016). Therefore, it is unsuitable for complex nonlinear data distributions. To take the non-linearity of data into account, CNN transforms input heatmaps to final representations, so-called feature vectors, which are separable by a linear clustering algorithm (van Elteren, 2018), i.e., CNN divides the different highlights of the heat maps for analysis and clustering. After this transformation step, we have a set of feature vectors used for K-means clustering.

We extracted the heatmap feature vectors by Google's InceptionV3 image analyzing deep neural network. It is trained on the ImageNet dataset which consist of millions of images used for object recognition, and image classification. For details about this dataset, we refer the reader to (Deng et al., 2009). Some features of Inception architecture are as follows (for more details refer to (Szegedy et al., 2016)):

- it is a module that typically has three types of different sizes of convolution and a maximum pooling.
- the channel is aggregated after the convolution operation in the previous layer for the network output. Then a nonlinear fusion is applied.

This architecture improves adaptability to different scales, and overfitting is better prevented (Kaur & Gandhi, 2020).

Transfer learning

As one increases the depth of the neural network, it will expand the number of parameters of the neural network. However, this improvement is at the cost of more computation resources and a larger dataset. To solve this issue, CNN based on transfer learning comes into the picture. Transfer learning lets us transfer the already trained model parameters to our new model and helps its training (Wang et al., 2019). After training on a large dataset, e.g., ImageNet, one can adopt transfer learning because CNN is able to learn generic features that are also applicable to other images without the need for training from scratch. Furthermore, the weights of the CNN, which is pre-trained on a large dataset, improve its accuracy for a specific task where the amount of available training data is limited (Iglovikov & Shvets, 2018), as stands for our data set.

Clustering evaluation

To calculate the goodness of clustering and select the appropriate number of clusters in the K-means method, we used the Silhouette Coefficient (Rousseeuw, 1987). The Silhouette ranges between -1 and 1, where high values show a well-matched point to its own cluster and poorly matched to the neighboring clusters. If many points have a negative value, the number of clusters needs to be modified. Silhouette Coefficient of point i is calculated as $s(i) = \frac{x(i)-y(i)}{max(x(i),y(i))}$ where, x is the average intra-cluster distance, and y is the average inter-cluster distance.

Furthermore, cluster analysis is an unsupervised learning problem, therefore a proper validation is of significant importance. Accordingly, two main types of validation criteria are introduced in the literature: internal and external (Rendón, Abundez, Arizmendi, & Quiroz, 2011; Jain, 2010). The internal criterion validates the the clustering based on the properties that are inherent to the data set. However, the external criterion validates based on the a priori information on the structure of the data, namely true labels (or ground truth). Such information is on the other hand usually either subjective or not available. Therefore, we used external criterion for evaluation of our clustering results. The qualitative metric of internal evaluation is visually assessing the similarity between clusters. The quantitative metric consist of the confidence interval of each cluster and evaluating how well the clusters are separated from each other. Also, comparing the overall area of different land-use types (derived from Open Street Map (OSM) (OpenStreetMap contributors, 2017) data) in the clusters help relating the resulting clusters to land-use types.

3. RESULTS AND DISCUSSION

We clustered the travel production heatmaps of the entire 1246 TAZs in the Netherlands, and calculated the Silhouette Score (SS) for various K values to determine the optimal amount of clusters. Our results suggest that the best cluster separation occurs when K=3 (see figure 3). Clustering the temporal patterns of production, using inception V3 with k-mean method, result in

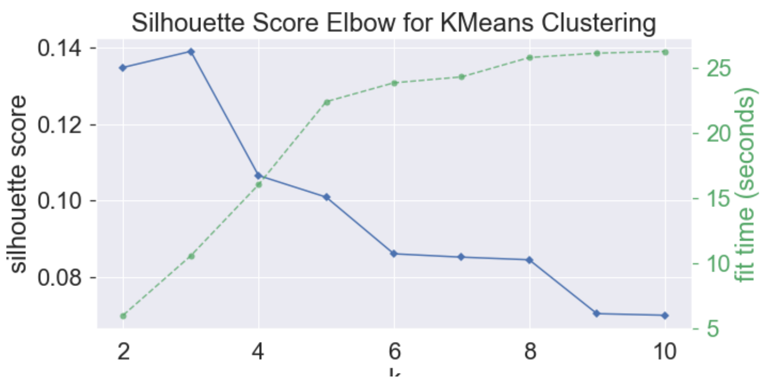

Figure 3: Silhouette Score for finding the optimum number of clusters.

the map shown in figure 4.

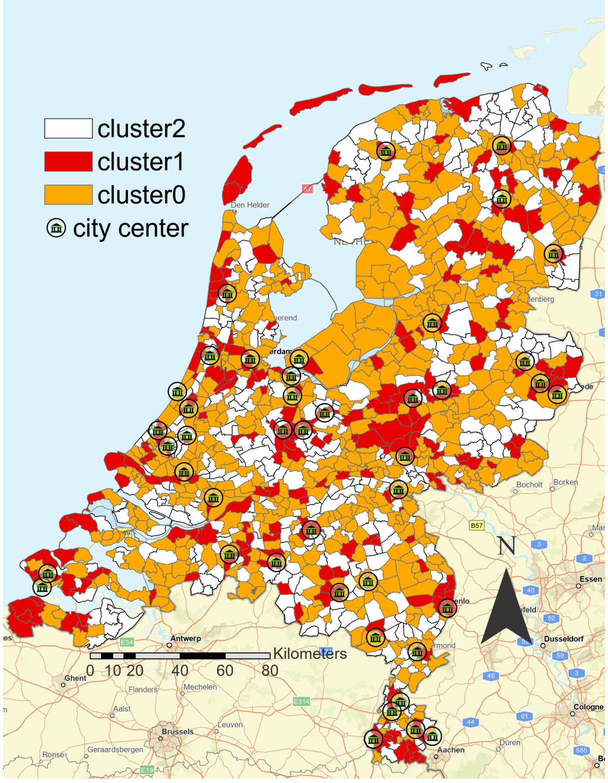

(a) **clusters and city centers.**

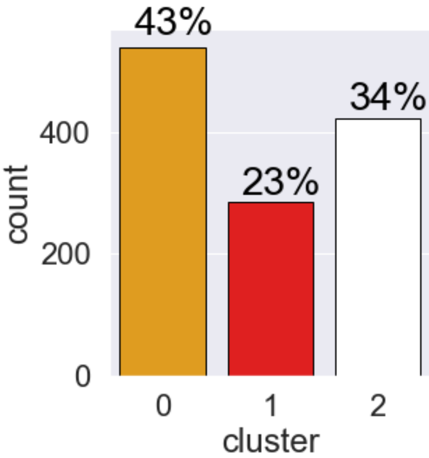

(b) **cluster share count.**

Figure 4: Travel production pattern clusters in the Netherlands.

Observing these three classes in space hints that zones in cluster1 which constitute a smaller proportion of zones (as shown in figure 4b), happen to be in more urbanized areas. In fact, as displayed in figure 4a, out of 43, 39 city centers fall into cluster1. Moreover, the obsolete areas are the least urbanized areas that happen to be in cluster2. The majority of farmlands also belong to this class. Comparing figure 4a with the land-use data of OSM (OpenStreetMap contributors, 2017) implies the following high density of features about cluster1:

- commercial and office buildings,
- rail and service roads,
- cycleway and footway,
- car and bicycle parking.

To look closer and quantify our claim, figure 5 shows that the majority of (50%) commercial/industrial areas, as a representation of urban areas, in the province of Utrecht belong to cluster1. Another representation (figure 6) shows that 48% of farmlands which are usually interpreted as rural areas fall into cluster2.

The above statements confirm that cluster1 reflects **urban**, cluster2 **rural**, and cluster0 **mixed-level** of urbanization area class. An analogy of the three clusters of temporal heatmaps of travel production is given in figure 7. Two of each cluster from various areas in the Netherlands are shown to see the similarities of the images inside the same cluster. Cluster1 (figures 7a and 7b), reflecting the urban class, has more severe afternoon peaks between 15:00 and 19:00 in producing trips. It can be due to more work-related land-use, i.e., people tend to leave work in the afternoon,

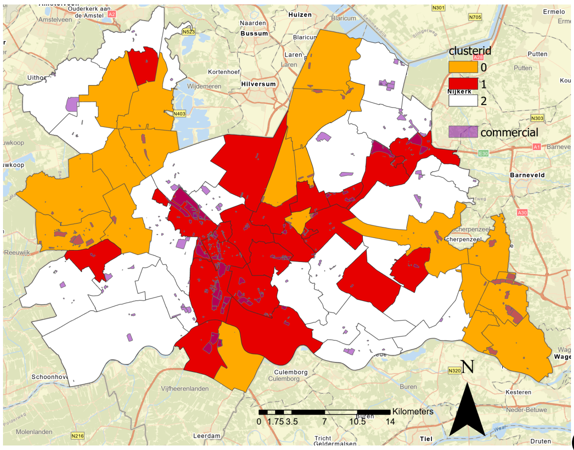

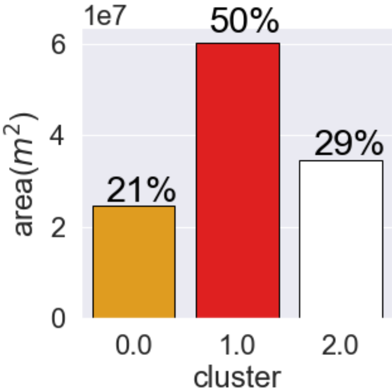

(a) commercial/industrial land-use.

(b) distribution of commercial/industrial area over the clusters.

Figure 5: share of clusters from commercial/industrial areas.

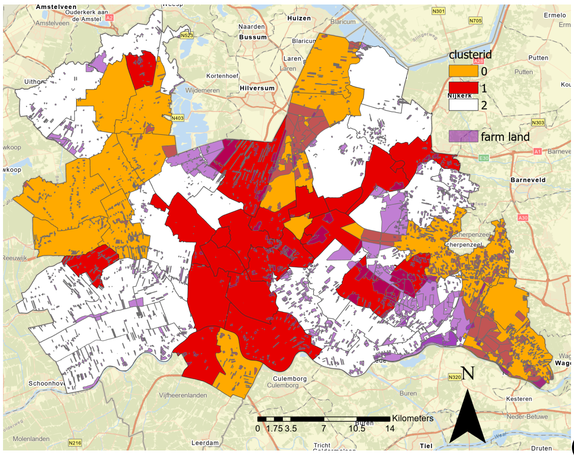

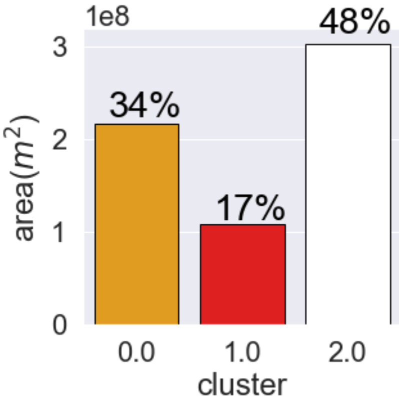

(a) farmland land-use.

(b) distribution of farmland area over the clusters.

Figure 6: share of clusters from farmland areas.

which causes a rise in the travel production of the urban places. Unlike the working days, weekends do not have significant peaks. The outliers of figure 7b might be indicating the non-regular patterns in that specific zone, which needs further analysis with longer intervals to confirm.

Cluster2 (figures 7c and 7d) which shows the rural class, displays more severe morning peaks from 06:00 to 09:00. It might be due to the dominancy of residential to work-related land use. In other words, people in residential areas mostly leave their house for their work (mostly located in urban areas) which causes extreme travel production values in the morning. Compared to the urban class in cluster1, the smaller peak interval reflects more scheduled activities (e.g., starting time of work) in the mornings and less obligation to leave urban zones (e.g., work) on time in the afternoons. Additionally, less regular activities like shopping and social events in the afternoon in metropolitan areas (i.e., cluster1) also trigger the longer peak range.

Cluster0 presents the patterns other than the ones in cluster1 and cluster2. For instance, in figure 7e, morning and afternoon peak seems almost equally extreme, which can be a presenter of suburb areas where a mix of residential and work land-use is established. Figure 7f, on the other hand, seems to be a weekend trip producer as some peaks are observed during the weekends and Friday afternoons.

Figure 8 gives insight into the average total hourly patterns of the travel production in each clus-

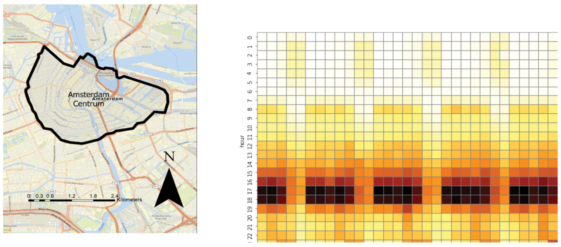

(a) cluster1

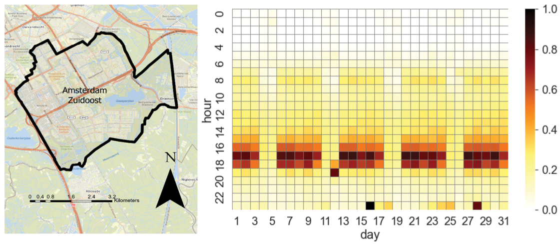

(b) cluster1

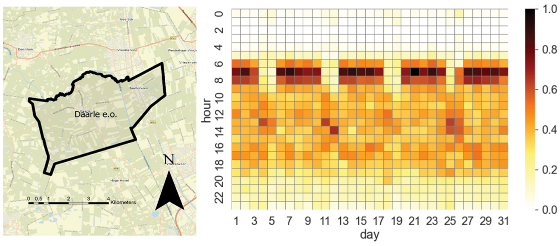

(c) cluster2

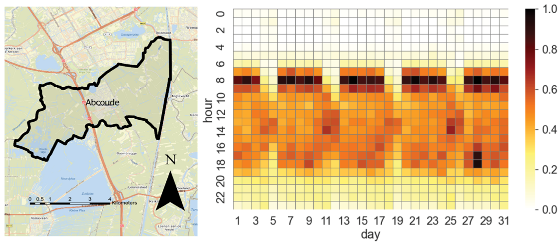

(d) cluster2

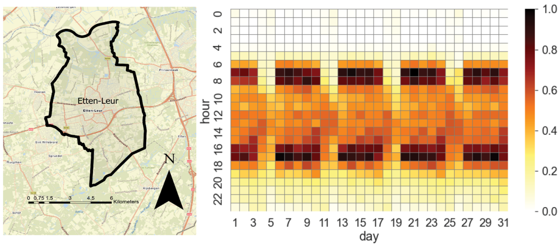

(e) cluster0

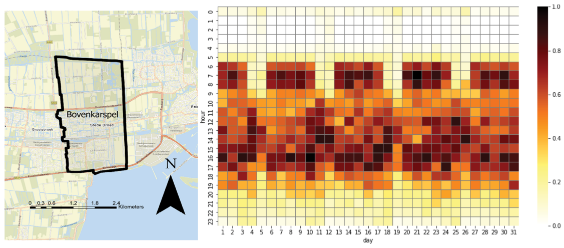

(f) cluster0

Figure 7: travel production clusters.

ter. The morning and afternoon peaks of all clusters seems to be almost at the same time range, however their difference in the production values are more significant during the afternoon peak. Figure 8a represents the line plots of 5% random sub-sampling of each cluster for 10 times. Ac-

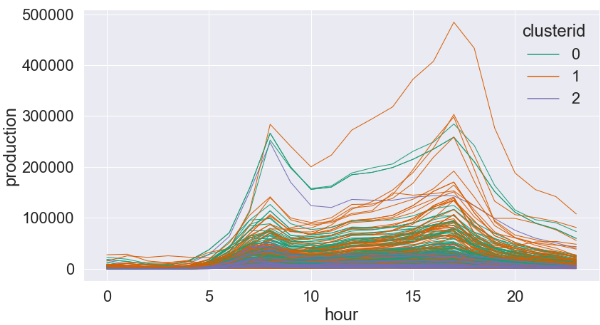

(a) with random 5% random sub-sampling for 10 times.

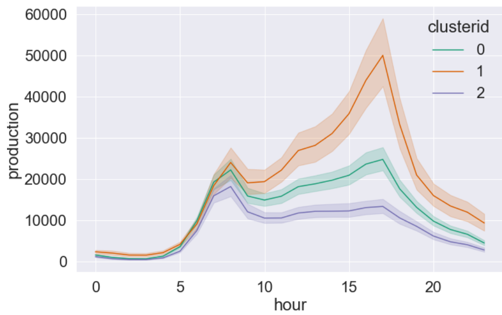

(b) with 95% confidence interval as the shaded area.

Figure 8: Average hourly production of the three clusters.

cordingly, the values are very widely scattered, especially in cluster 1, with higher average production in almost all day hours. In contrast, cluster2 representing the rural class, displays the lowest average production throughout a day. The shaded area in figure 8b represents the 95% confidence interval of average production, i.e., the 95th percentile of the distribution of the mean value for multiple (10,000) sub-samples. It shows that the estimated means of the clusters are robust and not sensitive towards the applied sampling to compute them. Moreover, the means of clusters are significantly different.

Figure 9 displays the average total daily pattern of the travel production in each cluster. In the

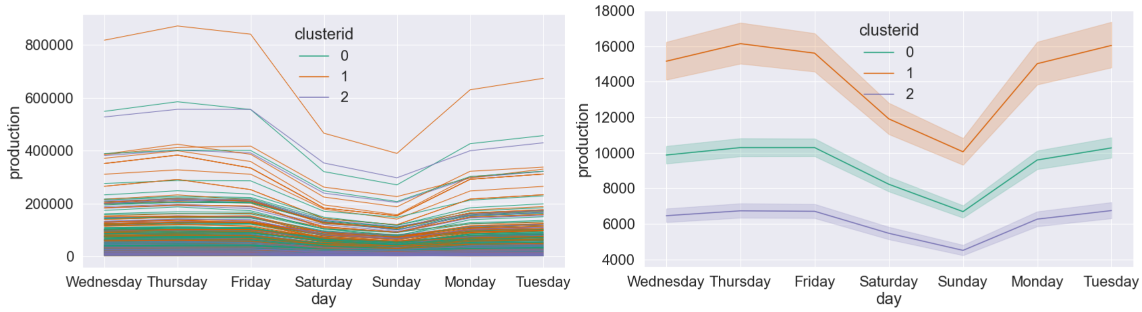

(a) with random 5% random sub-sampling for 10 times.

(b) with 95% confidence interval as the shaded area.

Figure 9: Average hourly production of the three clusters.

same way as hourly patterns, weekly average values seem to be robust estimates which imply (based on figure 9b showing the average confidence interval) well-separated clusters. However, figure 9a shows high variance meaning a widely scattered distribution of values. Moreover, the daily patterns seem very similar among all the clusters. A slight difference lies in the days with maximum averages. These are Thursday and Tuesday for cluster1, which indicates working areas. The days with maximum production for cluster0 and cluster2 are Tuesday, Thursday, and Friday, which can hint that work is not as dominant as it is in cluster1, i.e., as some part-time employees do not work on Fridays, having growth in the production values mainly indicates non-work-related trips.

4. CONCLUSIONS

The results presented in this paper describe the spatiotemporal patterns of travel production in TAZs of the Netherlands. The travel production of different areas reveals different temporal patterns within a day and between days. Clustering these patterns using a CNN based on transfer learning with the K-means method introduced three distinct clusters in the Netherlands. Observing these clusters in space and comparing them with the OSM land-use map suggested different urbanization levels for each cluster: urban, rural, and mixed-level. An urban area, which mainly presents the city center with a high density of urban facilities, reveals a sharp afternoon production peak indicating more work-related activities. However, a rural area shows more extreme production values in the morning, suggesting more residential. Mixed levels display other patterns in time and space. Our analysis shows that the three clusters have different average production, which is not sensitive to sampling. The analysis presented in this paper can be used in demand modeling studies to see the effect of urbanization on demand. Moreover, such analysis is required before using the processed demand data for policymaking and network development.

ACKNOWLEDGMENT

This research is sponsored by the NWO/TTW project MiRRORS under grant agreement 16270.

REFERENCES

Anselin, L., & Griffith, D. A. (1988). Do spatial effecfs really matter in regression analysis? *Papers in Regional Science*, *65*(1), 11–34.

Brunsdon, C., Fotheringham, A. S., & Charlton, M. E. (1996). Geographically weighted regression: a method for exploring spatial nonstationarity. *Geographical analysis*, *28*(4), 281–298.

Cardozo, O. D., García-Palomares, J. C., & Gutiérrez, J. (2012). Application of geographically weighted regression to the direct forecasting of transit ridership at station-level. *Applied Geography*, *34*, 548–558.

Cohn, R., & Holm, E. (2021). Unsupervised machine learning via transfer learning and k-means clustering to classify materials image data. *Integrating Materials and Manufacturing Innovation*, 1–14.

Deng, J., Dong, W., Socher, R., Li, L.-J., Li, K., & Fei-Fei, L. (2009). Imagenet: A large-scale hierarchical image database. In *2009 ieee conference on computer vision and pattern recognition* (pp. 248–255).

Fekih, M., Bonnetain, L., Furno, A., Bonnel, P., Smoreda, Z., Galland, S., & Bellemans, T. (2021). Potential of cellular signaling data for time-of-day estimation and spatial classification of travel demand: a large-scale comparative study with travel survey and land use data. *Transportation Letters*, 1–19.

Fotheringham, A. S., Charlton, M. E., & Brunsdon, C. (1998). Geographically weighted regression: a natural evolution of the expansion method for spatial data analysis. *Environment and planning A*, *30*(11), 1905–1927.

Gärling, T., Eek, D., Loukopoulos, P., Fujii, S., Johansson-Stenman, O., Kitamura, R., … Vilhelmson, B. (2002). A conceptual analysis of the impact of travel demand management on private car use. *Transport Policy*, *9*(1), 59–70.

Hartigan, J. A., & Wong, M. A. (1979). Algorithm as 136: A k-means clustering algorithm. *Journal of the royal statistical society. series c (applied statistics)*, *28*(1), 100–108.

Iglovikov, V., & Shvets, A. (2018). Ternausnet: U-net with vgg11 encoder pre-trained on imagenet for image segmentation. *arXiv preprint arXiv:1801.05746*.

Jain, A. K. (2010). Data clustering: 50 years beyond k-means. *Pattern recognition letters*, *31*(8), 651–666.

Kaur, T., & Gandhi, T. K. (2020). Deep convolutional neural networks with transfer learning for automated brain image classification. *Machine Vision and Applications*, *31*(3), 1–16.

Lin, J.-J., & Shin, T.-Y. (2008). Does transit-oriented development affect metro ridership? evidence from taipei, taiwan. *Transportation Research Record*, *2063*(1), 149–158.

Ma, X., Zhang, J., Ding, C., & Wang, Y. (2018). A geographically and temporally weighted regression model to explore the spatiotemporal influence of built environment on transit ridership. *Computers, Environment and Urban Systems*, *70*, 113–124.

Maat, K., & Timmermans, H. (2006). Influence of land use on tour complexity: a dutch case. *Transportation Research Record*, *1977*(1), 234–241.

Meppelink, J., Van Langen, J., Siebes, A., & Spruit, M. (2020). Beware thy bias: Scaling mobile phone data to measure traffic intensities. *Sustainability*, *12*(9), 3631.

Ning, C., & Hongyi, Z. (2016). An optimizing algorithm of non-linear k-means clustering. *International Journal of Database Theory and Application*, *9*(4), 97–106.

OpenStreetMap contributors, . (2017). *Planet dump retrieved from https://planet.osm.org.* Retrieved from https://www.openstreetmap.org

Poteraş, C. M., Mihăescu, M. C., & Mocanu, M. (2014). An optimized version of the k-means clustering algorithm. In *2014 federated conference on computer science and information systems* (pp. 695–699).

Rendón, E., Abundez, I., Arizmendi, A., & Quiroz, E. M. (2011). Internal versus external cluster validation indexes. *International Journal of computers and communications*, *5*(1), 27–34.

Rousseeuw, P. J. (1987). Silhouettes: a graphical aid to the interpretation and validation of cluster analysis. *Journal of computational and applied mathematics*, *20*, 53–65.

Shamos, M. I., & Hoey, D. (1975). Closest-point problems. In *16th annual symposium on foundations of computer science (sfcs 1975)* (pp. 151–162).

Shen, X., Zhou, Y., Jin, S., & Wang, D. (2020). Spatiotemporal influence of land use and household properties on automobile travel demand. *Transportation Research Part D: Transport and Environment*, *84*, 102359.

Szegedy, C., Vanhoucke, V., Ioffe, S., Shlens, J., & Wojna, Z. (2016). Rethinking the inception architecture for computer vision. In *Proceedings of the ieee conference on computer vision and pattern recognition* (pp. 2818–2826).

Thakuriah, P. (2001). Urban transportation planning: A decision-oriented approach. *Journal of Transportation Engineering*, *127*(5), 454–454.

van Elteren, T. (2018). *A comparative study of human engineered features and learned features in deep convolutional neural networks for image classification* (Unpublished doctoral dissertation).

Van Gansbeke, W., Vandenhende, S., Georgoulis, S., Proesmans, M., & Van Gool, L. (2020). Scan: Learning to classify images without labels. In *European conference on computer vision* (pp. 268–285).

Wang, C., Chen, D., Hao, L., Liu, X., Zeng, Y., Chen, J., & Zhang, G. (2019). Pulmonary image classification based on inception-v3 transfer learning model. *IEEE Access*, *7*, 146533–146541.

Xu, X., Chen, A., & Yang, C. (2017). An optimization approach for deriving upper and lower bounds of transportation network vulnerability under simultaneous disruptions of multiple links. *Transportation research procedia*, *23*, 645–663.

Yang, Z., Franz, M. L., Zhu, S., Mahmoudi, J., Nasri, A., & Zhang, L. (2018). Analysis of washington, dc taxi demand using gps and land-use data. *Journal of Transport Geography*, *66*, 35–44.